RSC Advances

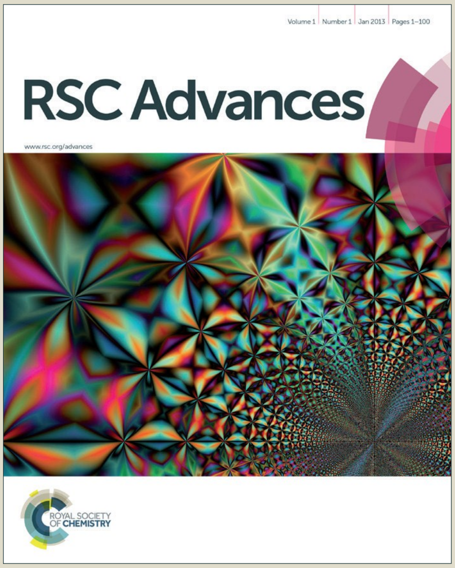

ROYAL SOCIETY
OF **CHEMISTRY**

www.rsc.org/advances

Graphical abstract

A Ternary Hybrid Nanoreactor with Thermoswitchable Catalytic Performance

Di Wang, Jie Hu*, Rong Zhao

Herein, a hybrid nanoreactor comprised of a mesoporous silica "head" and Poly(N-isopropylacrylamide) long chain "hairs" has been developed. The Ag nanoparticles contained in the regular channels of mesoporous silica are demonstrated a thermoswitchable catalytic characteristics, which is regulated by the temperature responsive organic long chains.

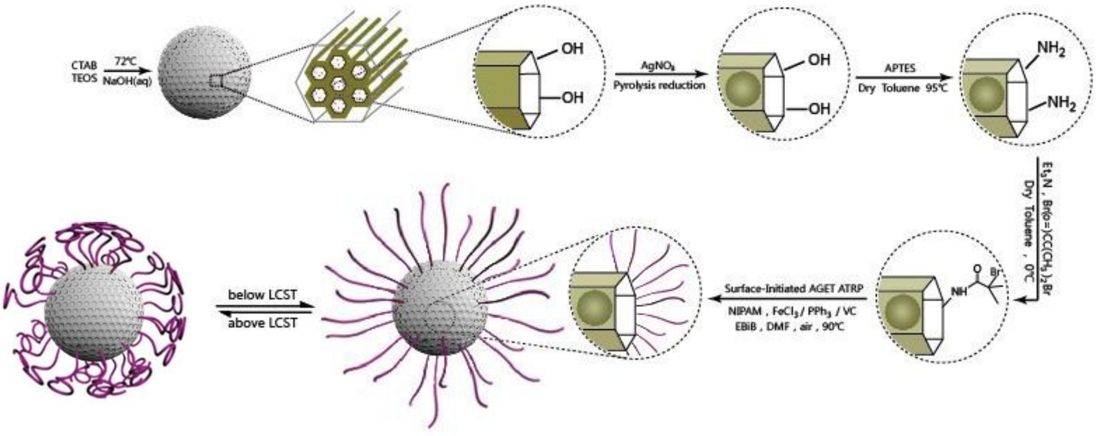

Scheme 1 Schematic presentation of the ternary hybrid nanoreactor with thermoswitchable catalytic performance and its preparation route

Cite this: DOI: 10.1039/c0xx00000x

www.rsc.org/xxxxxx

COMMUNICATION

A Ternary Hybrid Nanoreactor with Thermoswitchable Catalytic Performance †

Di Wang, Jie Hu*, Rong Zhao

Received (in XXX, XXX) Xth XXXXXXXXX 20XX, Accepted Xth XXXXXXXXX 20XX
DOI: 10.1039/b000000x

A hybrid nanoreactor comprised of a mesoporous silica "head" and Poly(N-isopropylacrylamide) long chain "hairs" has been developed. The Ag nanoparticles contained in the regular channels of mesoporous silica are demonstrated a thermoswitchable catalytic characteristcs, which is regulated by the temperature responsive organic long chains.

Lots of products, such as fine chemicals, medicines, polymers, and many other valued compounds important to humans, would not be feasible in the absence of catalysts. It becomes a shared belief now that manufacturing protocols can be made more economic, green, and sustainable by the design and wise use of catalysts[1,2]. In the recent years, nano-catalysis has attracted more and more interests as sustainable alternatives to conventional catalytic systems[3]. On the one hand, nano-sized catalysts, in many cases the noble metal nanoparticles (NPs), increase the exposed surface area of the active component, thereby enhancing the contact between reactants and catalyst dramatically, mimicking the homogeneous catalysts. On the other hand, their insolubility in reaction media renders them easily separated from the reaction mixture like heterogeneous catalysts[4]. Due to their high surface and consequently high surface energy, however, metal NPs tend to aggregate into clusters or larger particles, which leads to loss of the catalytic activity. To prevent NPs migration and the corresponding decay in the efficiency of the catalyst, different sorts of supporting materials, e.g. organic micelles[5,6], polymers[7,8] and inorganic materials[9,10], have been developed.

Among those supporting materials, smart polymers that can be switched "on" and "off" by external stimuli have attracted many attentions in recent years. They can not only isolate and protect the metal NP catalysts, but regulate effectively the reaction process and behavior under stimuli. Because changing temperature is relative easy in chemical reactions, temperature sensitive polymers are especially valuable in nano-catalysis. Lu and coworkers[11] reported an Au/poly(N-isopropylacrylamide) (PNIPAm) yolk-shell catalytic system. They found that the reaction rate of 4-nitrophenol catalysed by Au NPs at temperature below the lower critical solubility temperature (LCST) of PNIPAm was much higher than that at temperature beyond LCST. Using Ag NPs as catalyst and PNIPAm as thermo-sensitive supporting material, our group[12] constructed a shape memory reactor. This smart reactor indicated a tunable catalytic ability controlled by its temperature responsive shape change. It displayed a weak catalytic activity when curled to a roll at high temperature and a high activity if changed to an extended strip at low temperature. Recently, Monteiro *et al.*[13] designed a thermoresponsive polymeric nanoreactor in water capable of efficiently catalysing the aldol reaction to produce the product in high yields. The advantage is that cooling the reaction mixture below LCST of the polymer resulted in dissociation of the nanoreactor to fully water-soluble polymer chains and precipitation of pure aldol product from the nanoreactor. So the product could be isolated and collected very simply, just through centrifugation.

Although many important achievements have been obtained in this field, how to synthesize the nano-catalysts with controlled size, shape, morphology, and distribution in supporting materials is still a challenge. In this point, mesoporous silica becomes a better carrier candidate, owing to its regular channel structure, uniform pore size distribution, large surface area, and high chemical and thermal stability[14,15]. The uniform channels of mesoporous silica could facilitate the preparation of metal NP catalysts in a form with desired size and shape through an in-situ reaction of metal ions in the restrained cavities. Mesoporous silica, on the one hand, could effectively keep the catalysts stable even under harsh conditions because of its restrained space, high stability and good transportation; on the other hand, it also sufficiently expose the active surface of metal NPs to reactants because the NPs freely exist in the channels without the protection of any surfactant or polymer[16]. Furthermore, its silanol-containing surface can be easily functionalized with some intelligent molecules, allowing for a better control to respond to the external stimuli [17].

Combined the advantages of metal NPs, smart polymer and mesoporous silica, we herein report a ternary hybrid nanoreactor with thermo-switchable catalytic performance. As outlined in Scheme 1, briefly, the mesoporous silica nanoparticle (MSNP) with regular channel structures were prepared through a sol-gel reaction. Silver nitrate was used to form Ag NPs in cavities of MSNP by an in-situ reaction. Finally, utilizing an electron transfer activation and regeneration of atom transfer radical polymerization (ARGET ATRP), thermoresponsive PNIPAm long chains were grafted onto the surface of MSNP to get the ternary hybrid nanoreactor, Ag@MSNP-PNIPAm. When temperature is above the LCST of PNIPAm, the polymeric long chains grafted on the surface of the nanoreactor transit to hydrophobicity and shrink drastically in water, which results in the clogging of MSNP channels, consequently the difficult access of reactants in water to contact with Ag catalyst contained in MSNP. On the contrary, if temperature is below the LCST, the hydrophilicity of PNIPAm induces its extending conformation in water, which improves remarkably the availability of Ag NPs for reactants. As a result, using this novel smart nanoreactor, the catalytic reaction can be regulated effectively by temperature.

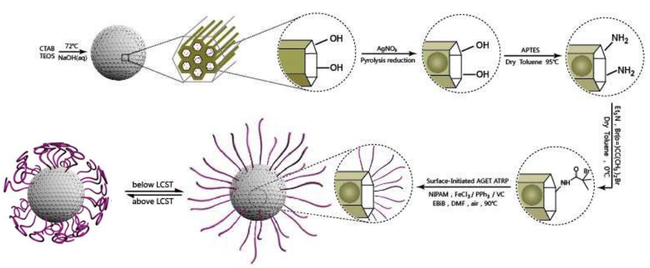

Scheme 1 Schematic presentation of the ternary hybrid nanoreactor with thermoswitchable catalytic performance and its preparation route

The FT-IR spectra of MSNP and Ag@MSNP-PNIPAm are shown in Fig. S1. Both of them indicate the Si-O-Si stretching vibration at around 1088, 954 and 803 cm^{-1}, showing that the silica framework of Ag@MSNP–PNIPAm remains unchanged after modification. However, contrary to MSNP, three characteristic peaks of PNIPAm at 3054 cm^{-1} (N-H stretching vibration), 1507 cm^{-1} (C=O stretching vibration) and 1208 cm^{-1} (C-N stretching vibration) are found in the curve of Ag@MSNP-PNIPAm, which demonstrates the successful grafting of the thermoresponsive chains onto MSNP. As can be seen from Table S1, the pore volume and pore size of Ag@MSNP-PNIPAm are 0.77cm^3/g and 9.72nm, respectively, both of which are just a little lower than those of MSNP. It seems that the modification don't significantly change the bulk structure of MSNP. Additionally, the Ag NPs contained in Ag@MSNP–PNIPAm are tested with XRD. As shown in Fig. S2, the peaks indexed to diffractions from the {1 1 1}, {2 0 0}, {2 2 0}, and {3 1 1} planes indicate existence of the face-centered cubic silver. Utilizing Debye-Scherrer equation, the particle size (D) can be calculated based on the XRD patterns:

$$D = k\lambda/\beta\cos\theta$$

Where k is the Scherrer constant; λ is the wavelength of the X ray; β is the peak width at half height; and θ is the Prague diffraction angle. So the average particle size of Ag NPs is evaluated to be about 12nm. As UV-Vis absorption spectroscopy is also an established method to characterize the formation of silver NPs[18], the UV-Vis spectrum of the smart nanoreactor was tested. It can be clearly seen from Fig. S3 that being different from MSNP, Ag@MSNP-PNIPAm exhibit an absorption peak in the range of λ_{max} = 450nm in the spectrum, the typical surface plasmon resonance band of Ag NPs. Furthermore, the surface plasmon resonance band in this region strongly suggests the formation of spherical particles[19]. To confirm the postulated spherical shape of the noble metal NPs and further investigate the morphology of the nanoreactor, transmission electron microscopy (TEM) experiments were carried out. It is found from Fig. 1(a) that the MSNP shows a spherical shape with the diameter in the range of 60-110nm. Most important, the hexagonal ordered pore structure with typical honeycomb appearance is demonstrated. Uniform channels run through the MSNP in parallel. From Fig. 1(b), in accordance with the UV-Vis data described above, spherical shape of silver NPs is observed. The size of Ag NPs is determined to be about 5-11nm, which is roughly agree with the result calculated from XRD data using Debye-Scherrer equation, as mentioned above. Profiting from the uniform channel structure of MSNP, silver NPs with small size and relative narrow size distribution are obtained, although a little aggregation occurs. Most interesting, all Ag NPs are found to be included inside the MSNP, which is an advantage for the stability, selectivity and activity of the catalyst. The content of the silver in the final product was determined to be about 4.5% (w/w), according to the weight changes when a given amount of MSNP was modified to Ag@MSNP and Ag@MSNP-PNIPAm. Elemental mapping images of Ag@MSNP-PNIPAm further demonstrated its ternary hybrid characteristics. As shown in Fig. S4, the occupied area of C element, only existing in the polymeric long chains, is much larger than that of Si element, which indicates that the PNIPAm chains graft on the surface of the MSNP and show an extended conformation at ambient temperature. For Ag element, contained in MSNP, a little aggregation is observed.

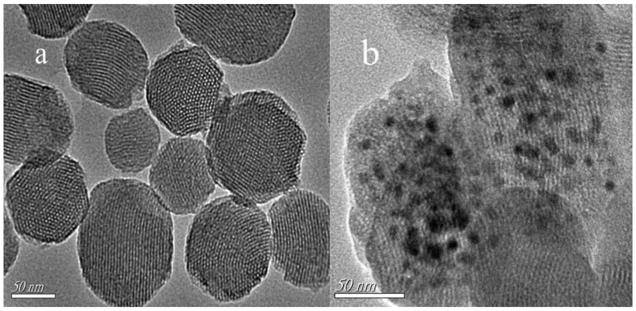

Fig. 1 TEM images of MSNP (a) and Ag@MSNP-PNIPAm (b)

Electrochemical studies were conducted to estimate the thermoswitchable "on/off" effects of PNIPAm chains for the MSNP channels. It is known that, for an electrochemical system with substrate molecules absorbed in nanoreactors, there are normally three steps involved in the electrochemical process: desorption, diffusion to the surface of electrodes, and terminal reaction[20]. The overall reaction rate in this system is thus determined by the slowest step, *i.e.*, the rate-determining step. In the case that the diffusion is eliminated with sonication, the overall reaction rate will directly rely upon desorption of substrate molecules from nanoreactors, considering the reaction of substrate on the surface of electrodes being fast. It is concluded that the potential to reduce/oxidize an absorbed substrate molecule depends upon the desorption constant. A difficult desorption will need more energy to overcome the blocking, thereby resulting in a larger redox potential[21]. As such, the electrochemical tests with substrate desorption were performed to follow the principle, where the nanoreactors were pre-absorbed with the reactant methylene blue (MB) and then placed into a cuvette encircled by a diffusion-eliminated sonication apparatus. Considering the temperature-sensitive characteristics of Ag@MSNP-PNIPAm, 25 ℃ and 45 ℃ are selected for a contrastive study, which are lower and higher than LCST of PNIPAm (≈32℃), consequently inducing the "on" and "off " states of channels of the smart nanoreactor, respectively.

As shown in Fig. 2, MB absorbed in Ag@MSNP-PNIPAm at 25℃exhibited a desorption/reduction peak at -120mv. In contrast, the desorption/reduction peak at 45℃ shifted to a higher position, -148mv. As expected, the Ag@MSNP-PNIPAm demonstrated a difficult desorption of MB at 45℃ than at 25℃, because of the shrinkage of PNIPAm chains "closing" the MSNP channels at the higher temperature. The self-switchable ability seems to play a key role for the desorption. In order to further investigate the desorption behaviours, Fig. S5 illustrates the desorption/reduction potentials of the reactant MB from the two control samples, namely MSNP-PNIPAm and MSNP. Just as anticipated, MSNP-PNIPAm revealed almost the same potential change with Ag@MSNP-PNIPAm (29mv and 28mv, respectively) in response to the increased temperature. In contrast, no significant shift of the desorption/reduction potential was observed for the MSNP when temperature changed. This result strongly suggests that the thermoresponsive PNIPAm chains can control effectively the “open” and “close” states of MSNP channels, thereby causing a switchable catalysis.

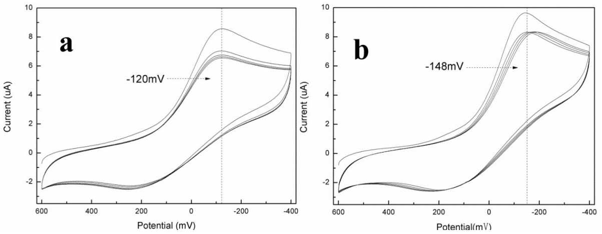

Fig. 2 DCV profiles with MB desorbing from Ag@MSNP-PNIPAm (a: 25℃; b: 45℃)

The catalytic property of the smart nanoreactor prepared is evaluated utilizing the reducing reaction of MB with $NaBH_4$ catalyzed by Ag NPs. To verify the thermoswitchable catalysis, two typical temperatures, 25℃ and 45℃, were also selected for the comparative study, like in electrochemical experiments. As indicated in Fig. 3, MSNP is found no obvious catalytic ability due to the absence of Ag NPs. In contrast, both Ag@MSNP and Ag@MSNP-PNIPAm showed significant catalytic activities and the conversions increased rapidly with time. However, although exhibiting catalytic ability, there was no controllable catalytic behavior being observed for Ag@MSNP, on which no PNIPAm chain was grafted. The little difference of conversion with temperature change is only because of the faster reaction rate at higher temperature. Most interesting, Ag@MSNP-PNIPAm indicated tunable catalysis as expected. After 20 min, the reaction conversion at 25℃, being 62.7%, is much higher than that at 45 ℃, only 20.4%. It is believed that hydrophobic phase transition and shrinkage of PNIPAm induced the blocking of MSNP channels, which make the difficulty of reactant molecules to contact with Ag NPs, should respond for the sharp decreasing of the reaction rate with temperature increasing.

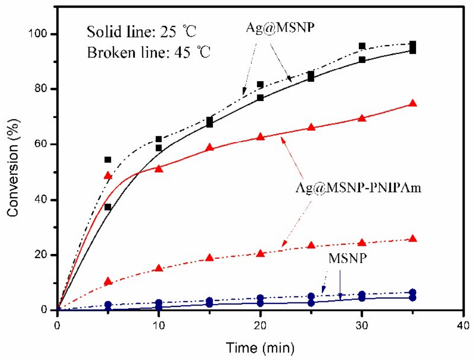

Fig. 3 Catalytic activity of Ag@MSNP-PNIPAm, Ag@MSNP, and MSNP at different temperature

The ability to repeat the switchable catalytic activity of Ag@MSNP-PNIPAm is shown in Fig. 4. The temperature was alternated between 25℃ and 45℃ for 8 times to estimate the repeatability of the smart nanoreactor prepared, in each which the conversion was tested after 10 min. It is found that the switching of the catalytic behavior of Ag@MSNP-PNIPAm was achieved and the catalysis can be made to repeatedly switch between both statuses. This result indicates that the switching catalytic statuses was reproducible and was dependent on whether the temperature was below or above the transition temperature of the thermo-responsive long chain grafted on MSNP.

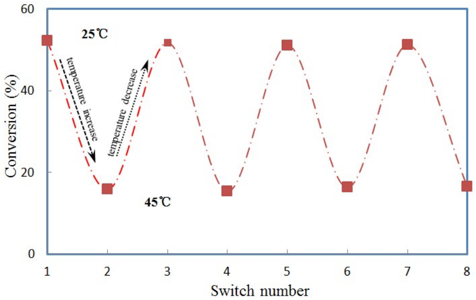

Fig. 4 Repetition of the switchable catalytic ability of Ag@MSNP-PNIPAm (the conversion was obtained for the reduction of MB with $NaBH_4$ after 10 min at different temperature)

In summary, a novel ternary hybrid nanoreactor was reported. Comprised of Ag NPs, MSNP and PNIPAm chains, this smart nanoreactor revealed thermoswitchable catalytic performance. The regular channel structure of MSNP facilitates the preparation of metal NPs in a desired form with small size and narrow size distribution. Electrochemical experiments demonstrated controllable desorption of substrate molecules upon temperature change. Most interesting, this smart nanoreactor indicated a tunable catalytic ability, which displayed weak reactivity at high temperature and high catalytic activity at low temperature. It is believed that the reversible extending and shrinkage of the PNIPAm chains grafted on MSNP surface upon the temperature change induced the corresponding switchable “on/off” variation. Therefore, it has been confirmed that controllable reactions can be realized by using this unique ternary hybrid nanoreactor composed of MSNP, noble metal NPs and thermo-responsive organic long chains, which opens up an opportunity to develop smart catalysts for complicated chemical processes.

Financial support of this study by China Postdoctoral Science Foundation (No. 2012M521007 and No.2013T60563) is gratefully acknowledged.

Notes and references

---

[a] *Institute of Polymer Materials, School of Materials Science and Engineering, Jiangsu University, Zhenjiang 212013, P.R. China. E-mail: hujiechem@hotmail.com; Tel/Fax: +86-511-88790191*

† Electronic Supplementary Information (ESI) available: Synthesis details, characterization and spectral data.. See DOI: 10.1039/b000000x/

1. L. Suljo, A. Umar, B. Calvin, and M. Matthew, *Nat. Mater.*, 2015, **14**, 567
2. Y. Zhu, and N. S. Hosmane, *Coordin. Chem. Rev.*, 2015, **293**, 357
3. V. Polshettiwar, and R. S. Varma, *Green Chem.*, 2010, **12**, 743
4. N. Tian, Z.-Y. Zhou, S.-G. Sun, Y. Ding, and Z. L. Wang, *Science*, 2007, **316**, 732
5. Y. Wei, S. Han, J. Kim, S. Soh, and B. A. Grzybowski, *J. Am. Chem. Soc.*, 2010, **132**, 11018;
6. Y.F. Shi, C.L. Tu, Q. Zhu, *Nanotechnology*, 2008, **19**, no. 445609
7. Y. Lu, M. Ballauff, *Prog. Polym. Sci.*, 2011, **36**, 767;
8. D. Diaz, D. Kuhbeck, R.J. Koopmans, *Chem. Soc. Rev.*, 2011, **40**, 427
9. M. Sanes-Sobrido, M. Perez-Lorenzo, B. Rodiguez-Gonzalez, V. Salgueirino, and M. A. Correa-Duarte, *Angew. Chem. Int. Ed.*, 2012, **51**, 3877
10. H. Wang, L. Chen, Y. Feng, and H. Chen, *Acc. Chem. Res.*, 2013, **46**, 1636
11. S. Wu, J. Dzubiella, J. Kaiser, M. Drechsler, X. Guo, M. Ballsuff, and Y. Lu, *Angew. Chem. Int. Ed.*, 2012, **51**, 2229
12. X. Wu, J. Hu, S. Li, R. Zhao, and D. Wang, *RSC Adv.*, 2014, **4**, 32063
13. H. A. Zayas, A. Lu, D. Valade, F. Amir, Z. Jia, R. K. O’Reilly, and M. J. Monteiro, *ACS Macro Lett.*, 2013, **2**, 327

14. J. Gu, J. Liu, Y. Li, W. Zhao, and J. Shi, *Langmuir*, 2013, **29**, 403
15. S. Huh, J. W. Wiench, J. Yoo, M. Pruski, and V. S.-Y. Lin, *Chem. Mater.*, 2003, **15**, 4247
16. X. Du, and J. He, *Micropor. Mesopor. Mat.*, 2012, **163**, 201
17. P. Yang, S. Gai, and J. Lin., *Chem. Soc. Rev.*, 2012, **41**, 3679
18. K. L. Kelly, E. Coronado, L. L. Zhao, and G. C. Schatz, *J. Phys. Chem. B*, 2003, **107**, 668
19. M. B. Ahmad, M. Y. Tay, K. Shameli, M. Z. Hussein, and J. J. Lim, *Int. J. Mol. Sci.*, 2011, **12**, 4872
20. S. Li, and S. Gong, *Adv. Funct. Mater.*, 2009, **19**, 2601
21. Y. Zhou, M. Zhu, and S. Li., *J. Mater. Chem. A*, 2014, **2**, 6834